

Crystal structure, phase stability, and magnetism in Ni₃V

J. -H. Xu* and T. Oguchi†

Department of Physics and Astronomy, Northwestern University, Evanston, Illinois 60201

A. J. Freeman

Department of Physics and Astronomy, Northwestern University, Evanston, Illinois 60201
and Materials Science Division, Argonne National Laboratory, Argonne, Illinois 60439

(Received 24 December 1986)

The structural phase stability and magnetism of Ni₃V are investigated using an all-electron total-energy local-(spin)-density approach for its cubic (*L*₁), tetragonal (*DO*₂₂), and hexagonal (*DO*₁₉) crystal structures. In agreement with experiment, the paramagnetic *DO*₂₂ structure is found to be the most stable phase. The *L*₁ structure shows a ferromagnetic instability with a magnetic moment of 1 μ_B per formula unit. An important role is found for the second-neighbor *d-d* coupling in determining the electronic structure and the observed crystal structure.

It is of considerable interest that the magnetic properties of Ni-V, Pd-V, and Pt-V alloys depend strongly on (i) the degree of atomic long-range order and (ii) the crystal structure. For example, VPt₃, which is paramagnetic in substitutionally disordered states with a face-centered-cubic lattice, becomes weakly ferromagnetic in ordered states with *L*₁ and *DO*₂₂ crystal structures. The absence of nearest-neighbor V-V pairs is believed to be responsible for the appearance of localized magnetic moments on the V atoms in these ordered alloys.¹ By contrast, VPd₃ has a tetragonal *DO*₂₂ crystal structure which is paramagnetic,² whereas a ferromagnetic state with a magnetic moment of 1.4μ_B per formula unit is predicted using a band-theoretical approach by Williams *et al.*³ for its cubic (*L*₁) structure. Burmester *et al.*² have suggested that for VPd₃ the discrepancy between the theoretical prediction³ and the experimental result² could be accounted for as be-

ing due to the V local environment. Bieber *et al.*⁴ studied the relative stability of the ordered transition-metal alloys in their *L*₁ and *DO*₂₂ ordered structures using the recursion method. Because the *DO*₂₂ structure can be obtained simply from the *L*₁ structure by introducing antiphase boundaries, they concluded that the density of states (DOS) could not be very different for both structures.

In the Ni-V alloys, the disordered alloys with up to 11 at. % V are ferromagnetic and are paramagnetic for higher concentration of V while the ordered Ni₂V and Ni₃V intermetallics show no magnetic order.⁵ The electronic structure of Ni₃V was calculated by Jaswal *et al.*^{6,7}

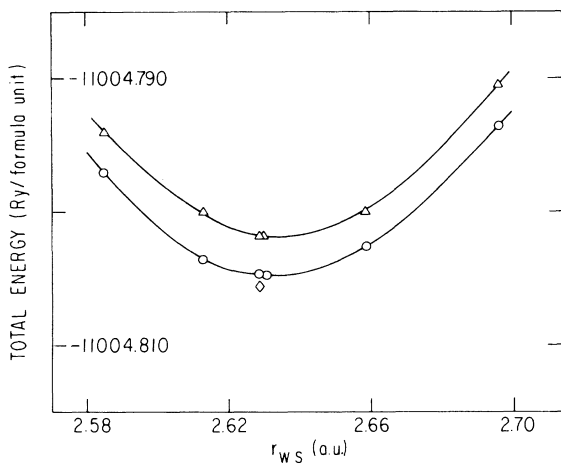


FIG. 1. Total energy as functions of the Wigner-Seitz radius and the number of *k* points within the $\frac{1}{48}$ IBZ for Ni₃V in the *L*₁ structure. Triangles, circles, and rhomboids denote calculated total energies with 30, 60, and 90 points, respectively.

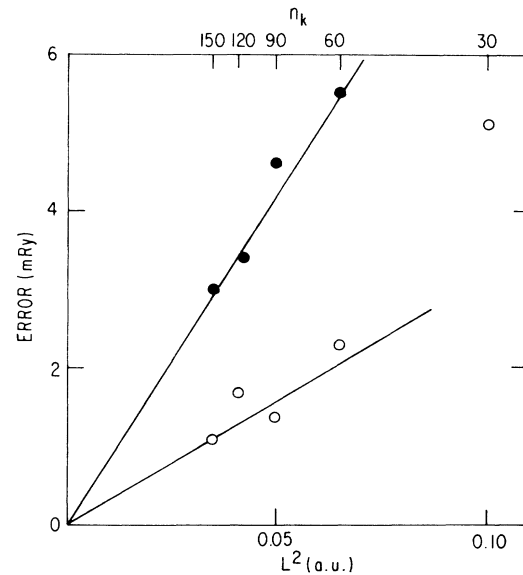


FIG. 2. Numerical error in the total energy resulting from the use of a finite number of *k* points in the Brillouin zone integrations for Ni₃V. *L* is a typical size of a tetrahedron in the linear tetrahedron scheme.

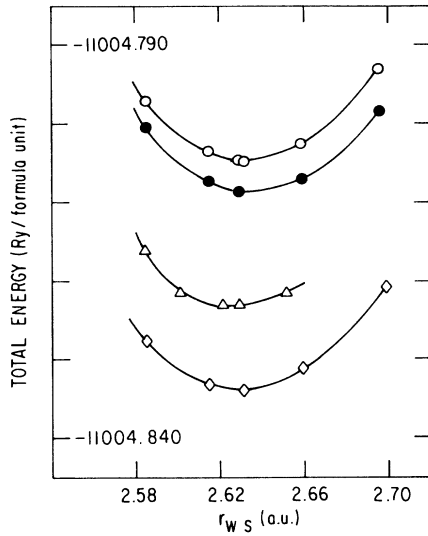


FIG. 3. Total energy as function of the Wigner-Seitz radius and its structure dependence for Ni_3V , using 60 k points within IBZ. Open and solid circles, triangles, and rhomboids indicate $L1_2$ (paramagnetic state), $L1_2$ (ferromagnetic state), DO_{19} and DO_{22} structures, respectively.

using the orthogonalized linear combination of atomic orbitals method and the linearized muffin-tin orbital (LMTO) method. They found that Ni_3V with the DO_{22} structure does not satisfy the Stoner criterion for ferromagnetic ordering. Their results showed that the overall feature of the calculated electronic structure is in good agreement with the angle-averaged photoemission spectra. A more detailed study of the dependence of the electronic structure and magnetism of the transition-metal-V compounds on different ordered structures is desired.

In the present paper, we investigate the structural stability and magnetism of Ni_3V by performing total-energy local-spin-density energy-band calculations for different crystal structures, cubic $L1_2$, tetragonal DO_{22} , and hexagonal DO_{19} . For solving the single-particle (Kohn-Sham) equations, the all-electron, semirelativistic LMTO method within the atomic-sphere approximation⁸ is employed. We find that a paramagnetic DO_{22} structure is most stable among the three different structures considered. Only the

$L1_2$ structure shows a ferromagnetic instability with a magnetic moment of about $1\mu_B$. However, the increase in the magnitude of the (negative) exchange energy found by introducing the magnetic moment in $L1_2$ is much smaller than the band-energy lowering due to the structural transition into the DO_{22} phase. Overall, an important role is found for the second-neighbor d - d coupling in determining the electronic structure and the observed crystallographic phase. In contrast to earlier conclusions,⁴ we find that the difference in DOS is partly due to the effect of differing second-nearest neighbors.

In carrying out the calculation we first examined the numerical precision of the total-energy approach. The total energy of cubic Ni_3V was calculated as a function of the lattice constant (expressed as the Wigner-Seitz radius) with 30, 60, and 90 k points within the irreducible wedge of the Brillouin zone (IBZ). The results are presented in Fig. 1. In general, the total energy has a lower value when calculated with the larger number of k points in the linear tetrahedron method. The error in the total energy depends on L^2 , where L is a typical dimension of a tetrahedron⁹ and $L \sim n_k^{-1/3}$ where n_k is the number of k points. As shown in Fig. 2, this L^2 dependence is roughly obeyed for smaller L values both for the $L1_2$ and DO_{22} structures. Thus, an accurate value of the total energy can be obtained simply by extrapolating the values of the total energy calculated with several different numbers of k points. It should be noted that we used such extrapolated values for calculations of the heats of formation. However, in the case of Ni_3V , 60 k points in the IBZ is enough to judge the stable state because the structural energy difference is much larger than the error due to the finite number of k points used.

The total energies are calculated as a function of the Wigner-Seitz sphere radius (r_{WS}) for paramagnetic Ni_3V in three different crystal structures, cubic $L1_2$, tetragonal DO_{22} , and hexagonal DO_{19} . The calculated total energies versus r_{WS} for these three structures are shown in Fig. 3 and the corresponding equilibrium Wigner-Seitz radii r_{WS}^0 bulk moduli and heats of formation¹⁰ are listed in Table I. For the $L1_2$ phase, the results of local spin density calculations for the ferromagnetic state are also given. Note that the ratio c/a was kept constant for the DO_{22} ($c/a=2.036$ which is the observed value¹¹) and DO_{19} ($c/a=0.816$ which is the ideal value of closed packing) phases.

TABLE I. The equilibrium lattice constants, Wigner-Seitz sphere radii, bulk moduli, and the formation energies for the three different structures ($L1_2$, DO_{19} , and DO_{22}) of Ni_3V .

Structure	a (Å)		c (Å)		r_{WS} (a.u.)	B (Mbar)	Formation energy (kcal/mole)
	Calc.	Expt. ^a	Calc.	Expt. ^a			
$L1_2$	3.55				2.633	2.3	11.2
DO_{19}	3.54		4.11		2.630	2.4	16.7
DO_{22}	3.54	3.5424	7.21	7.213	2.630	2.3	21.3

^aReference 11.

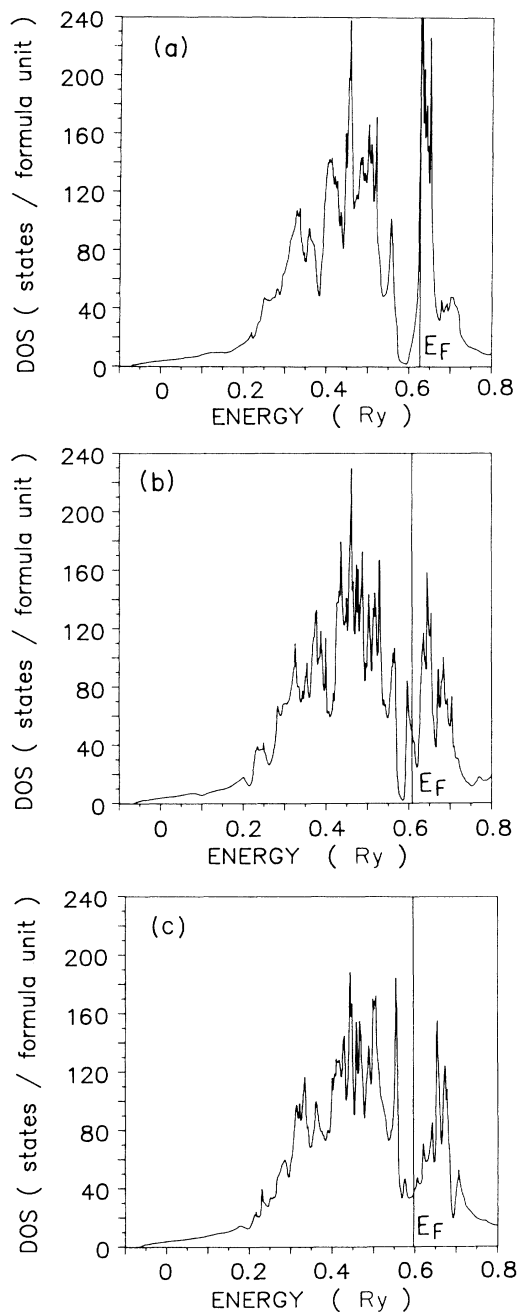


FIG. 4. Total density of states for Ni_3V ; (a) $L1_2$ structure; (b) DO_{19} structure; (c) DO_{22} structure.

Surprisingly, the calculated equilibrium Wigner-Seitz radii, r_{WS}^0 , for the different crystal structures are exactly the same within numerical precision, and are in excellent agreement with the observed radius of 2.632 a.u. (Ref. 11). As is clear from Fig. 3, the tetragonal DO_{22} structure is the most stable state among these three structures and the total energy is dramatically reduced when the structure changes from $L1_2$ to DO_{22} . The total energy of the DO_{22} structure is about 30 mRy per formula unit lower than that of the $L1_2$ structure and the total energy of the ferromagnetic state of Ni_3V ($L1_2$) is only about 4 mRy per formula unit lower than that of the paramagnetic state. Hence, the energy difference caused by the different crystal structure is nearly one order of magnitude greater than that due to magnetic effects. This can be understood from Fig. 4 which shows that the Fermi level of cubic Ni_3V lies on one of the peaks of the density of states. Therefore, it is expected that cubic Ni_3V , like cubic VPd_3 , will be more stable in the ferromagnetic state than in the paramagnetic state.

Overall, our calculated density of states (DOS) for the DO_{22} structure agrees well with that reported by Jaswal *et al.*⁷ but with our DOS value at E_F somewhat larger (2.68 states/eV formula unit) than theirs (2.54 states/eV formula unit), the Fermi level for the DO_{22} structure lies in a valley of the density of states curve [Fig. 4(c)]. The DOS at the Fermi level for the DO_{22} structure is reduced to about one fifth of that for the $L1_2$ structure (cf. Table II) which contradicts the conclusion of Bieber *et al.*⁴ Our spin polarized results yield a moment of $1.0\mu_B$ per formula unit for the $L1_2$ structure; this result is comparable to the value obtained by Williams *et al.*³ ($\sim 1.4\mu_B$ formula unit) for VPd_3 . Further, from the partial density of states (Fig. 5), it can be seen clearly that the density of states of Ni_3V is dominated by the d - d hybridization between V and Ni which depends strongly upon the atomic ordering (or crystal structure). Thus, although in both the $L1_2$ and DO_{22} structures each V atom is surrounded by twelve nickel atoms, the situation becomes different when the second-nearest neighbors are taken into account. Each V has two Ni and four V atoms as second-nearest neighbors in the DO_{22} structure compared to six V atoms in the $L1_2$ structure; therefore, the additional d - d interaction between Ni and V second nearest neighbors contributes to a stronger hybridization in tetragonal Ni_3V which can be

TABLE II. The total and partial density of states (projected by angular momentum and site) at E_F for the three different structures ($L1_2$, DO_{19} , and DO_{22}) of Ni_3V . (i) represents Ni sitting in (001) plane at the same layer as V, (ii) represents Ni sitting in (001) plane below or above V layer for DO_{22} structure.

Structure	Ni_s	Ni_p	Ni_d (states/Ry atom)	V_s	V_p	V_d	Total (states/Ry formula unit)
$L1_2$	0.64	5.01	23.99	0.06	3.58	100.68	193.23
DO_{19}	0.41	1.24	8.17	0.21	0.72	18.39	48.77
DO_{22}	(i)	0.17	1.85	8.26	0.18	0.89	12.46
	(ii)	0.14	0.94	5.27			36.51

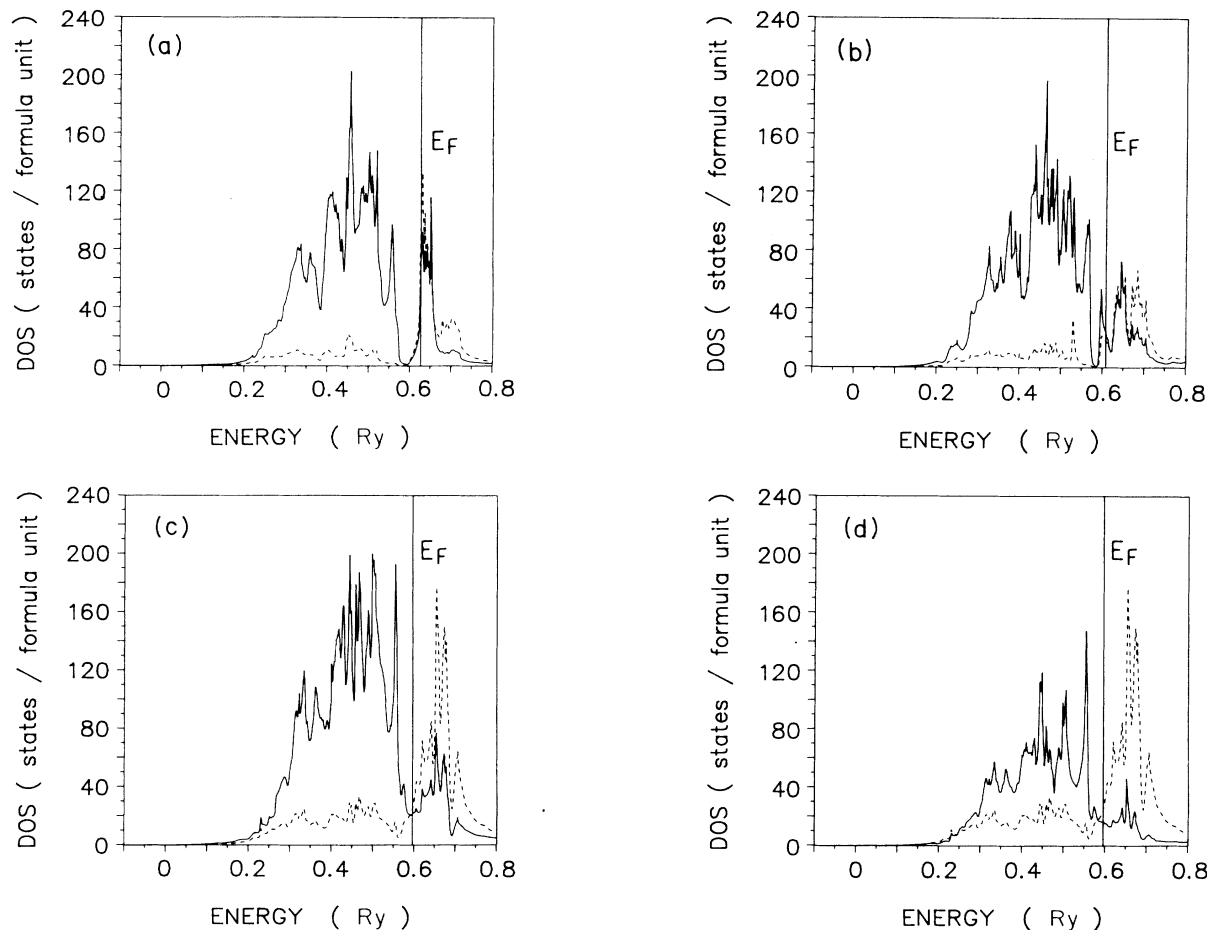


FIG. 5. Partial d density of states of Ni_3V . Solid line denotes Ni- d , and dashed line V- d . (a) $L1_2$ structure, (b) DO_{19} structure, and (c) and (d) DO_{22} structure; (c) represents Ni sitting in (001) plane at the same layer as V, and (d) represents Ni sitting in (001) plane below or above V layer.

seen qualitatively in Fig. 5.

In conclusion, the result of the total-energy calculation showed that in paramagnetic Ni_3V the tetragonal structure is clearly favored as compared to the cubic ferromagnetic structure. Thus, it is clear that as regards crystal stability, the (atomic) structure dominates the electronic structure, therefore magnetism.

ACKNOWLEDGMENTS

This work was supported by the Air Force Office of Scientific Research (Grant No. 85-0358) and the Department of Energy (including a grant of computer time on the BES CRAY computer). We are grateful to H. Lipsitt and D. Dimiduk for helpful critical discussions.

*Permanent address: Shanghai Institute of Metallurgy, Academy of Sciences of China, Shanghai 200050, China.

†Permanent address: National Research Institute for Metals, Nakameguro, Meguro-Ku, Tokyo 153, Japan.

¹R. Jesser, A. Bieber, and R. Kuentzler, *J. Phys. (Paris)* **42**, 1157 (1981).

²W. L. Burmester and D. J. Sellmyer, *J. Appl. Phys.* **53**, 2024 (1982).

³A. R. Williams, R. Zeller, V. L. Moruzzi, and C. D. Gelatt, Jr., *J. Appl. Phys.* **52**, 2067 (1981).

⁴A. Bieber, F. Ducastelle, F. Gautier, G. Treglia, and P. Turchi, *Solid State Commun.* **45**, 585 (1983).

⁵P. Turek and R. Kuentzler, *Physica* **107B**, 257 (1981).

⁶S. S. Jaswal, *Solid State Commun.* **52**, 127 (1984).

⁷S. S. Jaswal, D. J. Sellmyer, M. A. Engelhardt, and A. J. Arko, *Solid State Commun.* **57**, 223 (1986).

⁸O. K. Andersen, *Phys. Rev. B* **12**, 3060 (1975).

⁹H. J. F. Jansen and A. J. Freeman, *Phys. Rev. B* **30**, 561 (1984).

¹⁰The heat of formation is the energy difference between the compound and the weighted sum of the constituents, i.e., $\Delta E = E_{M_a X_b} - (aE_M + bE_X)$.

¹¹W. B. Pearson, *A Handbook of Lattice Spacings and Structures of Metals and Alloys* (Pergamon, New York, 1958).